40th AIAA/ASME/SAE/ASEE Joint Propulsion Conference and Exhibit
11 - 14 July 2004, Fort Lauderdale, Florida
AIAA 2004-4120

Images of Ground State Xenon Density in the Near Field of a Low Power Hall Thruster

Mark Cappelli#
Mechanical Engineering Department, Stanford University, Stanford, California

and

William Hargus, Jr.*
Electric Propulsion Laboratory, Air Force Research Laboratories, Edwards AFB, California

Measurements are presented of the qualitative distribution of neutral ground state xenon in the near field of a 200W Hall thruster. The diagnostic employed is a variation of a classical absorption technique, applied at the vacuum ultraviolet wavelength of the 147 nm resonance transition of XeI, using retro-reflected intrinsic resonance line emission as a source for re-absorption. This method has, in principal, the sensitivity of a narrow-band absorption diagnostic, with a limitation due largely by the accuracy in the return beam alignment. The main drawback in this method is in making the diagnostic quantitative, as the analysis requires knowledge of the broadening mechanisms of the resonance line, and a re-construction of the spatial signals to account for the non-uniform distribution of absorbers. The results, though qualitative, reveal some unexpected features in the near-field, which we attribute to the interaction of the neutral xenon discharged from the thruster with the background xenon chamber gas.

I. Introduction

The plasma near-field of Hall thrusters is the subject of much research. In the near-field, within a few thruster diameters, and in the vicinity of the cathode, electron transport is poorly understood, the presence of the precipitous "cone-jet" is yet to be explained, and the role of chamber gas ingestion on overall plume structure has not been very well characterized. While plasma properties such as electrostatic potential, temperature, and ion velocities can be measured using either electrostatic probes or laser probing of excited electronic states of xenon, the density of the neutral xenon ground electronic state is still rather elusive. This is largely due to the low densities ($\sim 10^{18}$ m^{-3}) and inaccessibility by optical probing as a result of the large excitation energy (8.5 eV). Knowledge of the neutral xenon density in the near field is paramount to the development of thruster simulations, in particular, if one is attempting to capture the current-voltage behavior of the thruster discharge.

This paper describes a preliminary characterization of xenon density field obtained in the near-field of a 200W Busek Hall thruster, operating in Chamber 6, at the Air Force Research Laboratory (AFRL) Electric Propulsion Research Facility at Edwards Air Force Base. The approach taken is to measure the radiative transfer characteristics of the intrinsic resonance transition ($5p^6$ (^1S_o) – $5p^5 6s$ ($^3P_1$)) centered at 146.97 nm. This measurement required the application of vacuum ultraviolet spectroscopy. Details of the theory and experimental approach are given below.

II. Background

The most straightforward method of measuring xenon ground state atomic species number density, n_{Xe}, is by absorption spectroscopy. With this method, broadband or narrowband radiation about the $5p^6$ (^1S_o) – 6s

Associate Professor, Mechanical Engineering Department, Stanford University, and Member, AIAA
*Senior Research Scientist, Electric Propulsion Laboratory, Air Force Research Laboratory, and Senior Member, AIAA

Copyright © 2004 by the American Institute of Aeronautics and Astronautics, Inc. All rights reserved.

($^3P_1$) transition in neutral xenon (XeI) at 146.97 nm is passed through the plasma plume of the Hall thruster, in the near field of the exit plane. The transmitted radiation is imaged onto the entrance slit of a vacuum monochromator or straight onto a photodetector. The intensity of the transmitted beam relative to that incident onto the plasma is a direct measure of the number of absorbers present. Knowledge of the detailed optical constants (e.g., line strength and broadening rates) makes this an absolute measurement not necessarily requiring calibration for physical constants. In principal, there is no limit to the sensitivity that can be achieved in this measurement, although experimental drifts and finite integration times (to overcome photon statistics) limits these types of absorption measurements on atomic resonance lines to densities above about 10^{18}-10^{20} m^{-3}. In the case of the 147 nm resonance transition in xenon, the fact that this wavelength lies in the vacuum ultraviolet (VUV) region of the electromagnetic spectrum makes this particularly difficult, in that it requires use of either a stable, broadband source in the VUV, or a narrow xenon resonance lamp that is not in itself self-absorbed.

The absorption strategy that we used in this study is referred to here as a reflection – reabsorption method. This method is a variation of a narrowband absorption technique performed using the intrinsic emission from the plasma that is being probed, as the spectrally-narrow probe beam itself. In applying this strategy, a measurement is made of the (spectrally unresolved) emission associated with the resonance transition. The signal associated with this is referred to as the direct emission, S_{DE}. This emission may be optically thick for the line of interest, and, for a uniform plasma source, could have a distorted spectral shape that asymptotically approaches the Planck distribution beginning near its spectral line center. A second measurement is made of the resonance emission that propagates in the opposite direction but reflected so that it retraces its path through the plasma into the optical path used for emission. The spectral signature of this emission source will be characterized by reduced intensity near the transition line center, owing to absorption by the neutral xenon. The signal associated with this is referred to as the reflected emission, S_{RE}. In practice, both measurements are made simultaneously, using optics shared by both paths. The measurements are coincident, and are distinguished from each other by using phase sensitive detection. A chopper is used to modulate the direct emission at a frequency ω_{DE} while a second chopper is used to modulate the reflected emission at a frequency ω_{RE}. Two lock-in amplifiers serve to separate the signals on a single detector. The ratio of the signal $R = S_{RE} / S_{DE}$ is a function of the ground state neutral xenon number density. The major drawback of this method is that measurements can only be made of a luminous plasma (since its emission serves as the probe itself). This did not prove to be an impediment here, in the measurements where confined to the annular plasma region of the near field of a coaxial Hall thruster.

In the background theory described here, it is assumed that the background xenon in the chamber does not contribute to the absorption of the resonance line in either of the two branches. The effect of the background pressure will serve to reduce the signals S_{RE} and S_{DE}. In the actual analysis of the data, the background density must be taken into account. The background number density is sensitive to the ratio S_{RE} / S_{DE} detected at large distances off axis. In the absence of background xenon, this ratio should approach unity, as both paths should lead to optically thin radiative transport.

The spectral irradiance emitted by hot plasma of <u>uniform excitation temperature</u>[¶] but <u>non-uniform absorption coefficient</u> along a direction z, over a path length L is [1]:

$$I_{\omega_{DE}} = I_{\omega_P}\left(1-\exp\left(-\int_0^L \kappa_\omega dz\right)\right) \qquad [1]$$

Here, I_{ω_P} is the Planck function, which describes the isotropic thermal radiation field at the excitation temperature of the resonance state, and κ_ω is the spectral absorption coefficient for the resonance transition ($1 \rightarrow 2$), which is given as:

¶ The assumption of a uniform excitation temperature greatly simplifies the analysis, and, based on probe measurements at the exit of Hall discharges, is expected to lead to only a small error in the measured density, in comparison to other experimental uncertainties.

$$\kappa_{\omega} = \frac{h\omega}{8\pi^2} B_{12} N_1 \phi_{12}(\omega) \qquad [2]$$

N_1 ($\approx n_{Xe}$) is the ground state xenon number density, ϕ_{12} is the transition lineshape, and B_{12} is the Einstein stimulated absorption coefficient, given as:

$$B_{12} = \frac{4\pi^3 e^2 f_{12}}{\varepsilon_o h m_e \omega_{12} c} \qquad [3]$$

where f_{12} = 0.264 [2] is the transition absorption oscillator strength, and all other symbols represent the usual atomic constants.

The resonance transition lineshape is assumed to be Doppler, resonance, and lifetime-broadened. It is noteworthy that the resonance transition in xenon is subject to hyperfine splitting due to electron angular momentum coupling to the nucleus, as well as isotopic shifting due to variations in the term energies for different isotope masses. For spectral features that are much broader than the hyperfine structure, the hyperfine structure can be considered as an additional broadening component. The optical constants associated with these shifts are largely unknown for this transition, though a recent study by Anderson et al [2] assigns the broadening associated with this transition to < 0.9 cm^{-1}, and probably closer to about 0.1 cm^{-1}. Our preliminary analysis presented in this paper find that the estimated xenon densities are moderately sensitive to the estimated hyperfine structure, and a value of 0.9 cm^{-1} was used for the purpose of a preliminary analysis of early results [3]. Here, we review the basic theory, simplified for a uniform plasma, and use these results to present a qualitative interpretation of new experimental data, rendered in the form of *line density images*. As you will see, even though these images are qualitative, they provide insight into the complex structure of the near-field. A future analysis will examine the effects of hyperfine splitting in more detail, account for the non-uniform nature of the flow, and will attempt to render these images to be more quantative.

If the spectral irradiance given by Eqn. [1] is redirected back through the plasma, then this irradiance serves as a background source, which will be further attenuated in accordance with Beer's Law:

$$I_{\omega_{RE}} = I_{\omega_P}\left(1-\exp\left(-\int_0^L \kappa_{\omega} dz\right)\right)\exp\left(-\int_0^L \kappa_{\omega} dz\right) \qquad [4]$$

At this point, some simplifications are noteworthy, and, for the purpose of a preliminary analysis which describes the usefulness of this diagnostic, are warranted. As mentioned above, we shall assume that the plasma is uniform along the length L, and that over the spectral range of the transition, the Planck function does not vary substantially. Both of these conditions can (indeed, must) be relaxed, for a more detailed analysis but serve to illustrate the usefulness of this diagnostic here. Also, we shall integrate over a spectral bandwidth, $\Delta\omega$, as it is assumed that the monochromator involved in isolating the resonance transition serves primarily as a spectral filter (i.e., does not scan over the emission/absorption feature to resolve the structure). Under these circumstances, Eqns. [1] and [4], when spectrally integrated, reduce to:

$$I_{DE} = I_{\omega_P}(\omega_{12}) \int_{\omega_{12}-\Delta\omega/2}^{\omega_{12}+\Delta\omega/2} \left(1-\exp\left(-\kappa_{\omega}(\omega)L\right)\right) d\omega \qquad [5]$$

$$I_{RE} = I_{\omega_P}(\omega_{12}) \int_{\omega_{12}-\Delta\omega/2}^{\omega_{12}+\Delta\omega/2} \left(1-\exp\left(-\kappa_{\omega}(\omega)L\right)\right) \times \exp\left(-\kappa_{\omega}(\omega)L\right) d\omega \qquad [6]$$

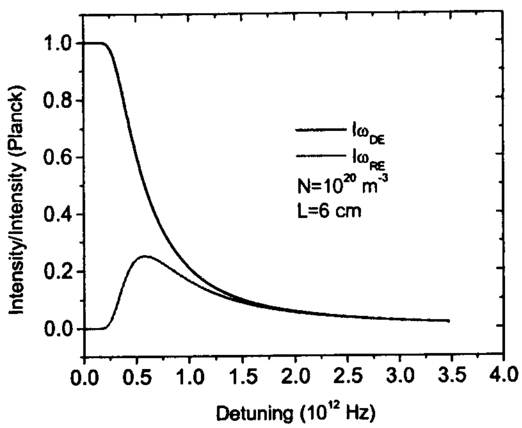

Figure 1: Spectral shape of the directly emitted spectral line ($I_{\omega DE}$), and of the reflected ($I_{\omega RE}$) resonance line that is re-directed through the uniform 6 cm - long path of plasma.

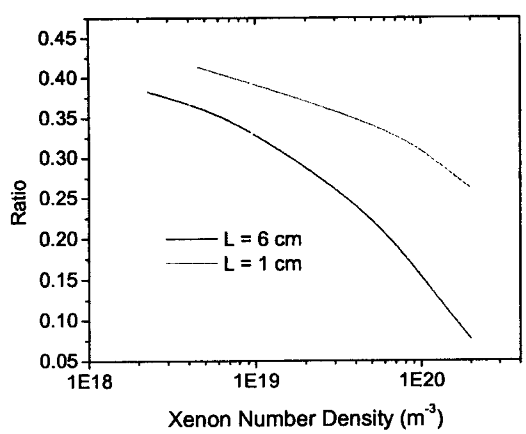

Figure 2: Integrated intensity ratio, R, with C_R=1, as the background neutral xenon number density is varied. Shown are calculations for 1000K and two cases of neutral xenon path length: L = 6 cm, and L = 1 cm.

The actual signals detected will be proportional to some geometric, spectral, and electronic conversion factors, G_{DE} and G_{RE}, which can be different for the two branches.

The signal ratio:

$$R = \frac{S_{RE}}{S_{DE}} = C_R \frac{I_{RE}}{I_{DE}} \quad [8]$$

with $C_R = G_{RE} / G_{DE}$ a constant that can be determined, as discussed above, by evaluating the ratio as it passes through a chord of the co-axially symmetric Hall discharge plasma that is either very short ($L \to 0$), or is optically thin to the emitted and reflected spectral line ($\kappa_\omega L << 1$). However, this ratio is expected to be unity only in the absence of absorption due to background xenon in the chamber. Since there is a finite amount of background xenon in the chamber (some 10^{-6} Torr during operation), a calibration must be performed using spectral emission lines (e.g., from boron (BI) or for ionized xenon (XeII)) that are expected to be optically thin.

For purposes of illustration, we plot in Figure 1, the normalized spectral irradiance (integrands of Eqns. [5] and [6]), $I_{\omega_{DE}} / I_{\omega_P}(\omega_{12})$ in 2a) and $I_{\omega_{RE}} / I_{\omega_P}(\omega_{12})$ in 2b) that is expected to be directly emitted and re-transmitted through the plume. In this example calculation, we have assumed a xenon gas temperature of 1000K, a plasma path length of L = 0.06 m, and a xenon ground state number density of $N = 10^{20}$ m^{-3}. It is apparent that while the direct emission saturates near the spectral line center to the Planck radiation limit, the reflected emission that is re-transmitted through the plasma suffers re-absorption and the depletion of its spectral line core. The ratio of the integrated emission for these two cases (assuming C_R = 1), as the ground state xenon density is varied, is given in Figure 2. We see that the ratio varies modestly with xenon gas density, and depends on the path length (as expected), rendering this measurement suitable as a diagnostic over the expected xenon density range. Indeed, it appears as though there is an approximate linear relation between the inverse ratio, *1/R*, and the number density, lnN_1, i.e.,

$$\ln N_1 \approx C \frac{S_{DE}}{S_{RE}} \quad [9]$$

As we shall see below, we use this to qualitatively map the neutral xenon number density variation in the near field of the thruster plume. Because the broadening is dominated by the hyperfine splitting, the ratio is not found to be very sensitive to the gas temperature.

For regions very close to the exit plane, the model may not be appropriate, as the neutral density should occupy a ring coincident with the channel dimensions that correspond to the location of the inner and outer channel walls, respectively, and so a quantitative analysis based on a uniform plasma assumption is not valid. Nonetheless, the maps show some interesting qualitative features that have not yet been discussed in the literature.

III. Experiments

The Hall thruster studied here belongs to the family of Busek BHT-200 thrusters, which nominally run at a power of approximately 200W. It has an inner wall diameter of 15 mm, and an outer wall diameter of 31 mm (8 mm channel width). The central pole piece extended approximately 7 mm beyond the exit plane of the channel. The tip of the pole piece served as the origin position marker for the axial position referred to in the measurements. The cathode was located approximately 20 mm downstream of the central pole piece. The chamber used at AFRL is 1.8 m in diameter and 3 m long with a measured pumping speed of ~ 32,000 l/s on xenon, provided by four single-stage cryo panels and one 50 cm diameter two-stage cryo-pump.

A 2.54 cm diameter MgF_2 lens inside the tank having an effective focal length of 26.87 cm (and positioned 26.87 cm from the thruster geometric center) served to collect and collimate the direct emission, which is chopped for phase-sensitive detection at a frequency ω_{DE}. In the first variation of this diagnostic [3], a second lens of the same characteristics collects the same emission along a direction opposite to that of the direct emission, collimates it and redirects it back to retrace its path through the plasma using an ultraviolet sensitive mirror. This lens and mirror were subsequently replaced by a 25 cm focal length VUV mirror placed 50 cm from the thruster centerline, with approximately 80% reflectivity at 140 nm. This emission then falls on the first lens, and is re-collimated to be coincident with the path of the direct emission. In order to distinguish this resonance emission from the direct emission, it is chopped at a different frequency, ω_{RE}. Both the direct emission and the reflected emission, which are collimated while inside the chamber, are focused onto the entrance slit of a ¾ m vacuum monochromator using a 21 cm focal length, 2.54 cm diameter MgF_2 lens. A continuous vacuum interface is facilitated through the use of flexible vacuum bellows, which support the lens. Other dimensions (e.g., placement of choppers) are not critical. For the measurements described here, the entrance and exit slits of the monochromator were set to approximately 100 μm, providing a spectral resolution of approximately 0.1 nm. A solar blind photomultiplier is used to provide a signal proportional to intensity falling on the exit slit. This signal is sent to the lock-in amplifier for further analysis.

Experiments were carried out after careful alignment of the optical paths for concentricity, with the vacuum chamber open. The thruster was operated at nominal conditions (I = 0.82 A, V = 250V, mass flow rate = 8.5 sccm (anode), 1 sccm (cathode)). During operation under these conditions, the background pressure as recorded by an ionization gage (uncorrected for xenon) was typically about 5×10^{-6} Torr. For the results presented here, the emission path traverses the plume at an axial position z defined by the distance away from the tip of the conically shaped cone. The thruster is translated laterally (along a direction normal to the thrust axis and emission path) so that the emission traverses laterally across the plume along various chords.

IV. Results

Representative signal maps from both the direct emission and the reflected retransmitted emission are shown in Figure 3, taken with the thruster operating at nominal conditions. Overlays depicting the location of the thruster and the cathode are included in the figures. These are spatial scans taken by lateral (vertical) and axial (horizontal) translation of the Hall thruster, with interpolation and rendering carried out in Matlab©. It is apparent that the overall spatial variation in the direct emission is much different than that of the reflected emission. The direct emission shows considerable spatial structure, such as strong toroidal emission in the vicinity of the thruster channel, and strong emission in the vicinity of the cathode orifice. In addition, there appears to be a strong and abrupt rise in emission downstream of the cathode, reminiscent of a weak compression in the flow, though such structures are not anticipated in these very rarefied conditions. The reflected emission has fewer features and appears as a strong homogeneous emission source between the exit plane and the cathode. It is particularly interesting that these images have little or no resemblance to the appearance of the plume in the visible region of the spectrum, as seen by the eye, which is the result of optically thin radiation between excited electronic states of both neutral and ionized xenon.

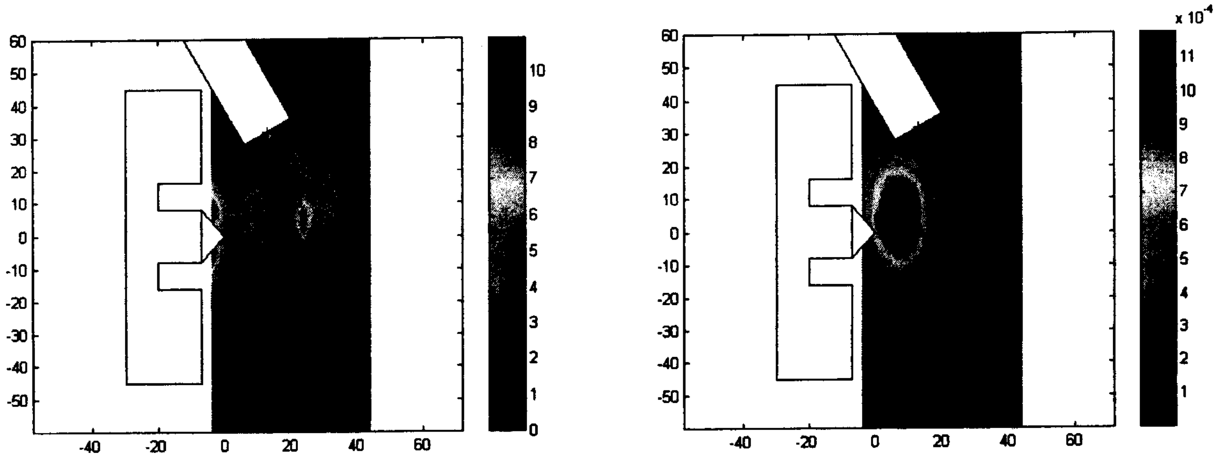

Figure 3. Maps of the Direct Emissions (left) and Reflected-retransmitted Emission (right) for nominal discharge conditions.

Figure 4 presents the ratio of the two maps shown in Figure 3, which should track the variations in the xenon number density, in accordance with Eqn. [9] above. This ratio has not been corrected for relative path sensitivity. It appears, from this map, that there is a rapid drop in the density at the exit of the channel, but a sudden, rather abrupt increase in the density some 20 mm from the channel exit, in the vicinity of the cathode plane. The regions at large lateral positions (beyond ~ 40 mm from the axis should be interpreted with caution, as the signal levels (in both direct and reflected emission) drop precipitously at these locations.

The map shown in Figure 4 does indicate that there is a rapid expansion of the neutral xenon plume beyond the channel, and provides very compelling evidence of a possible affect associated with either the interaction of the plasma exiting the thruster with: (a) the cathode jet, or (b) the background xenon in the chamber.

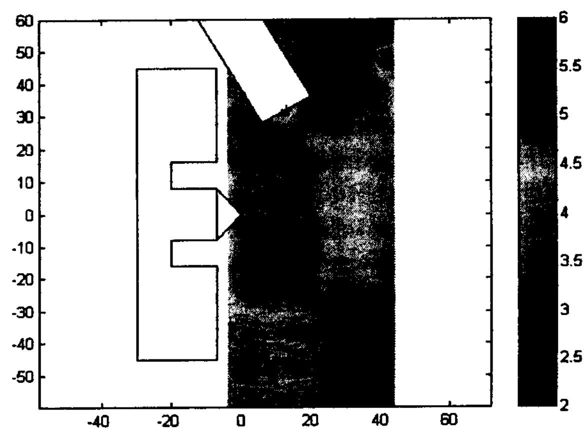

Figure 4. Map of the signal ratio in the Direct (DE) and Reflected (RE) emission. This map qualitatively features the spatial variation in the number density, in accordance with Eqn. [9] in the text.

In order to help us understand the structure in these maps, experiments were carried out under conditions similar to those of Fig.4, but with a substantially increased mass flow rate through the cathode (to 3 sccm from 1 sccm). It is noteworthy that this increase led to a 12% increase in anode current. The resulting map of xenon density is shown in the top frame of Figure 5 below. There is a noticeable asymmetry in the plume, with increased signal in the region of the cathode. Also apparent is the presence of a high density layer, which was only a subtle feature at the lower flow rates.

The lower frame in Fig. 4 shows the qualitative image of the near field neutral density when the background chamber pressure was increased by about 25% by bleeding additional xenon into the chamber. The result was a substantial increase in the signal in the very near region of the exit plane, and a sharpening in the rise in density at a location of approximately 40 mm from the exit plane of the thruster. The reason for this sharp increase in density is yet unclear. It is possible that there is an interaction of the rarified neutral xenon beam with the background chamber gas which leads to a slight compression.

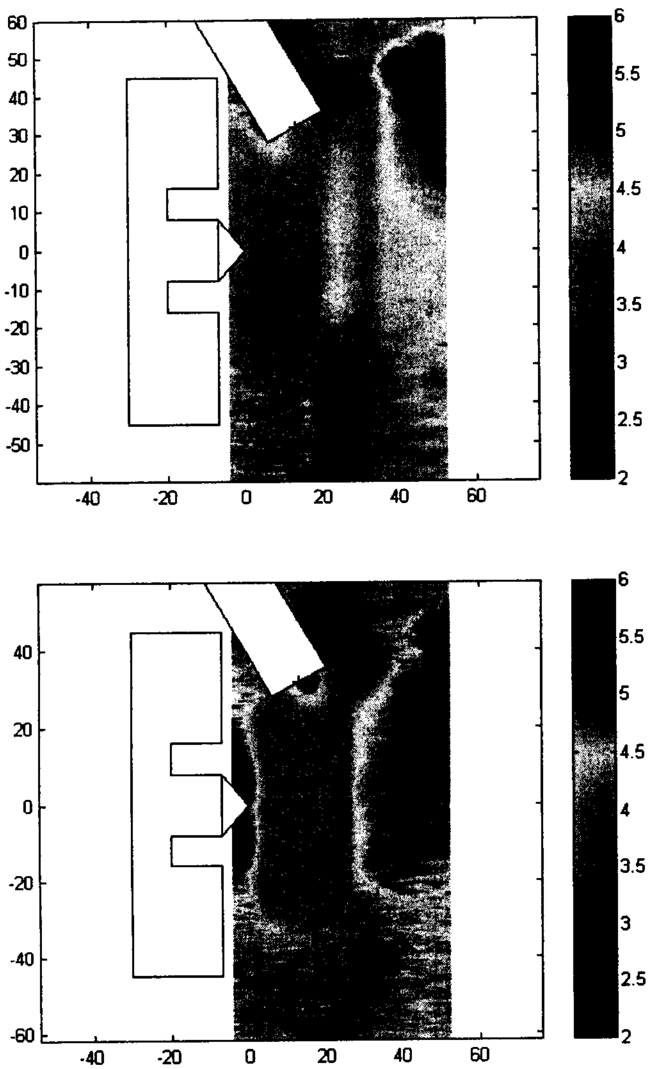

Figure 5. Qualitative map of the spatial variation in the number density, similar to that of Fig. 4: **Top** – tripling of the mass flow rate of xenon through the cathode. **Bottom** - 25% increase in chamber pressure (6.7 x 10^{-5} Torr).

The apparent variation in near-field structure with increased chamber pressure is nonetheless an indicator that even at this relatively low chamber pressure, the limited pumping speed of even some of the better ground test facilities can alter the structure of the plume in the near field of these Hall discharges.

V. Summary

This paper describes a preliminary measurement of the qualitative distribution of neutral ground state xenon in the near field of a 200W Hall thruster. The diagnostic employed is a variation of a classical absorption technique, applied at the vacuum ultraviolet wavelength of the 147 nm resonance transition of XeI, using retro-reflected intrinsic resonance line emission as a source for re-absorption. This method has, in principal, the sensitivity of a narrow-band absorption diagnostic, with a limitation due largely by the accuracy in the return beam alignment. The main drawback in this method is in making the diagnostic quantitative, as the analysis requires knowledge of the broadening mechanisms of the resonance line, and a re-construction of the spatial signals to account for the non-uniform distribution of absorbers. The results, though qualitative, reveal the presence of unexpected features, such as a sudden expansion (drop in density) within a discharge chamber diameter downstream of the thruster, followed by an abrupt rise in density just downstream of the cathode plane. The rise in density is attributed to a weak compression due to the interaction of the unionized portion of the plume, with the background chamber gas. The spatial field is seen to be moderately dependent on the cathode xenon flow rate, and the background chamber gas pressure.

Acknowledgements

The measurements were taken at the Air force Research Laboratories (Edwards Air Force Base). Support for Mark Cappelli was provided by the Air Force and the National Academy of Science through a summer faculty fellowship. The authors would like to thank Nicolas Gascon for his assistance in the image renderings.

References

1. Griem, H.R., in Plasma Spectroscopy, (McGra w Hill, New York), 1964, p. 174.
2. Anderson, H.M., Beregeson, S.D., Doughty, D.A., and Lawler, J.E., Phys. Rev. **A 51**, 211, 1995.
3. Cappelli, M.A., and Hargus, W.A. Jr., Paper AIAA-2003-5007, AIAA Joint Propulsion Conference, Huntsville, AL July 20-23, 2003.